Case Studies in Thermal Engineering 23 (2021) 100813

Contents lists available at ScienceDirect

Case Studies in Thermal Engineering

journal homepage: http://www.elsevier.com/locate/csite

Melting performance enhancement of thermal storage system by utilizing shape and position of double fin

Nazaruddin Sinaga [a,**], Hazim Moria [b], Kottakkaran Sooppy Nisar [c], Cuong Manh Vu [d,***], Behzad Heidarshenas [e], Akbar Arsalanloo [f], Mohammad Mehdizadeh Youshanlouei [f,*]

[a] Mechanical Engineering Department, Engineering Faculty of Diponegoro University, Jalan Prof. Soedarto, SH Tembalang, Semarng, Central Java, Indonesia
[b] Department of Mechanical Engineering Technology, Yanbu Industrial College, Yanbu Al-Sinaiyah City, 41912, Saudi Arabia
[c] Department of Mathematics, College of Arts and Sciences, Prince Sattam Bin Abdulaziz University, Wadi Aldawaser, 11991, Saudi Arabia
[d] Institute of Research and Development, Duy Tan University, Danang, 550000, Vietnam
[e] College of Mechanical and Electrical Engineering, Nanjing University of Aeronautics and Astronautics, Nanjing, PR China
[f] Sustainable Management of Natural Resources and Environment Research Group, Faculty of Environment and Labour Safety, Ton Duc Thang University, Ho Chi Minh City, Vietnam

ARTICLE INFO

Keywords:
Vertical PCM enclosure
Double fins
Triangular fin
Fin shape
Fin position
Lauric acid

ABSTRACT

In present study, a 2D rectangular enclosure was considered as a latent thermal energy storage (LTES) system. Lauric acid was used as PCM material. The aim of this study was to use fins to enhance melting process of PCM. Position and shape of double fins were considered as investigating parameters. At first stage three different positions were considered for fins of rectangular shape. Results indicated that amongst aforementioned cases, best results were achieved when double fins were located at lower half of enclosure. Results revealed that up to 1800s could be saved during whole melting process. At second step, two trapezoidal form and one triangular shaped double fins were used to evaluate the effect of fin shape. In these cases, fins were placed at optimum position concluded from previous stage. Results presented that up to Fo = 0.15, best values of Nusselt numbers were related to triangular shaped fins. After Fo = 0.15, the case with triangular fin has least Nu number. The best melting performance was related to triangular fins at which 1000s less melting time was observed. Enhancement ratio results presented better performance for triangular fins after second of 2500s.

1. Introduction

Due to human population growth and industrial developments, demand for energy has raised sharply in recent decades [1]. Lack of sufficient energy sources and high price of energy necessitates the efficient consumption of energy [2]. Different methods as like to

* Corresponding author.
** Corresponding author.
*** Corresponding author.
E-mail addresses: nsinaga19.undip@gmail.com (N. Sinaga), moriah@rcyci.edu.sa (H. Moria), n.sooppy@psau.edu.sa, ksnisar1@gmail.com (K.S. Nisar), vumanhcuong@duytan.edu.vn (C.M. Vu), behzadheidarshenas@nuaa.edu.cn (B. Heidarshenas), akbar.arsalanloo@gmail.com (A. Arsalanloo), m.mehdizadeh.y@yahooo.com (M.M. Youshanlouei).

https://doi.org/10.1016/j.csite.2020.100813
Received 26 October 2020; Received in revised form 7 December 2020; Accepted 11 December 2020
Available online 17 December 2020
2214-157X/© 2020 The Authors. Published by Elsevier Ltd. This is an open access article under the CC BY-NC-ND license (http://creativecommons.org/licenses/by-nc-nd/4.0/).

using renewable energies [3], utilization methods [4] and the use of thermal energy storage technologies have gained considerable attractions [5]. Sensible thermal energy storage, thermochemical thermal energy storage and latent thermal energy storage (LTES) are of three types of energy storage systems [4]. The LTES with PCMs (phase change materials) because of great repeatability [6], controllability [7], significant density [8] of energy storage and nearly Isotherm discharging process [9], are used in various applications such as heat recovery systems [10]of automotive waste [11], utilization of solar energy unites [12] and etc. However, the low thermal conductivity of PCM unites is a very important disadvantage [13]. This feature extends duration of melting time and decreases the efficiency of PCM systems [14]. With the aim of solving this issue, researchers have proposed various methods [15]. Many have worked on inserting various types of fins to augment heat transfer in PCMs [16–19], some have worked on adding single [20,21] and hybrid [22] nanoparticle additives to PCMs for their thermal conductivity enhancement while others have proposed using multiple PCMs to increase the charging and discharging rates [23,24]. Porous media is another solution suggested in the literature which can enhance conductivity of the PCM [25,26]. Some experts have adopted more creative methods by combining two of the approaches mentioned above such as inserting fins along with adding nanoparticles to enhance performance of system [27,28].

Amongst aforementioned enhancement methods, the use of fins due to their easy manufacturing method and low cost are widely used in PCM systems [29]. Fins increase the heat transfer area and the produced heat in the heat source easily transfers from high conductive material (metal fin) to low conductive material (PCM). Besides the presence of fins could affect the intensity of buoyancy driven motion of the melted PCM which results in more quick melting process [30]. Effect of the presence of fins on the thermal performance of a PCM based heat sink were investigated by Hosseizadeh et al. [31]. They investigated the effect of different parameters as like to fin thickness, fin height and number of fins. Their results presented that by increasing the fin height and number, the thermal performance of the PCM unite significantly increases. Also, they found that the effect of increment of thickness of the fins on the thermal performance of thermal storage unite was minor. Ji et al. [32] studied the effect of inclination angle of double rectangular fins on the performance of vertical rectangular PCM enclosure. They considered five inclination angles of 0°, $+15^\circ$, $+30^\circ$, -15°, and -30°. Their results indicated that double fins with downward inclination angle of -15° has more effect on melting performance of PCM enclosure. It was found that by using double fins with inclination angle of -15°, the total melting time could decease up to %23.8. Cao et al. [33] investigated the effect of fins through annular PCM unite. Through their study, they tried to find the optimal number of longitudinal fins. They found that for a certain wall temperature the number of fins has an optimal value. They mentioned that ten fins could have the most effective influence on decreasing the melting time of the horizontal annular PCM unite. Joneidi et al. [34] experimentally analyzed the effect of various configuration of fins on the melting process of a horizontal rectangular enclosure. They proposed an empirical correlation for the prediction of melting fraction during the melting process. Abdi et al. [35] investigated the effect of vertical fins on the melting performance of horizontal PCM enclosure. They stated that despite of horizontal configuration of fins, the vertical fins do not suppress the buoyancy driven motion of melted PCM which would lead in more improvement of the melting process. Jinlong et al. [36] performed a numerical study and investigated the effect of structure, metaling volume fraction and fin orientation on the melting performance of a PCM unite which was designed for thermal management of mobile electronics. Tian et al. [37] studied the effect of material of the metal fin on the thermal performance of PCM Unite. The fins material was made of steel302, aluminum, copper and carbon steel. Their results presented that by using copper made fins, the total melting time of the PCM unite could decrease up to %41.7. Yıldız et al. [38] presented a new and three like branching fins and analyzed the melting performance of PCM enclosure. They considered different aspect ratios and length to height ratios of rectangular fins. They found that optimizing the geometrical properties of rectangular fins could be more effective than utilizing the triangular fin.

In this study, a 2D rectangular enclosure was considered for simulating the melting process of PCM. Generally, vertical latent heat storage systems are used in thermal managements of buildings. They help to diminish energy consumption, postpone the load of thermal peaks, facilitate temperature control in building parts, and increases their durability [39]. At the first stage the location of rectangular fins was studied. At the second stage the shape of rectangular fins was changed to trapezoidal form. At the final stage, triangular double fins were used for further improvement of thermal performance of the considered PCM unite. Parameters as like to melting fraction, surface averaged Nusselt number, melting contours and etc. are analyzed.

Based on the literature review and according to the authors' best knowledge, there is no previous study that considers the effect of location of rectangular fins on melting of PCM. In this study firstly, effect of location of fins on melting of PCM has been studied to find the optimized case and secondly, the shape of fins in the optimized case was enhanced and trapezoidal and triangular fins were employed for further optimization of melting process in the PCM.

2. Problem statement and solution methods

2.1. Physical model

The computational model consists of a two-dimensional rectangular enclosure with its height and width being equal to 50 mm. The double fins attached to a heater plate have been placed on the left wall of the enclosure. The thickness of heater plate is 5 mm and left wall of heater plate is isothermally heated at constant temperature of 343 K. The position of fins has been altered in different cases to find the most efficient state for melting rate of PCM. Later, trapezoidal and triangular shaped fins were employed to further enhance the heat transfer. Lauric acid and aluminum have been used as the material for PCM and the fins respectively which their properties have been presented in Table 1. The initial temperature of PCM is equal to the ambient temperature which is 298.15 K.

The study has been conducted in three stages. At first step effect of location of fins is evaluated on the melting of PCM. In second step the optimum state evaluated in the first step is selected to study the heat transfer characteristics of trapezoidal fins and finally triangular fins have been employed for heat transfer enhancement and PCM melting optimization. It is to be noted that to make the

results comparable, the heat transfer surface in all of the above cases needs to be equal. As the computational domain is 2 dimensional and the length of 3rd dimension normal to the plane of model is considered to be unit, the length of base of the fins and the circumferential length of the fins in all of the cases have been considered to be equal. The dimensions and configuration of different cases studied have been depicted in Fig. 1 schematically.

2.2. Mathematical methods

The flow conditions are considered to be laminar and unsteady. Also, the liquid PCM is regarded as an incompressible and Newtonian fluid with neglecting its volume expansion during the phase change process. To simulate the phase change process, the Enthalpy-Porosity technique proposed by Voller and Prakash [41] is employed. In this method, the mushy region is considered as a porous medium in which the volume fraction at each cell represents its porosity. In this method the fully solidified regions are assigned to the porosity of zero and fully melted regions are assigned to the porosity of 1. To account for the reduced velocity resulted from the solidified material, a source term is added to the momentum equation. According to the assumptions made, the governing equations including continuity, momentum and energy equations can be expressed as:

$$\frac{\partial \rho}{\partial t} + \nabla \cdot (\rho \vec{u}) = 0 \tag{1}$$

$$\frac{\partial}{\partial t}(\rho \vec{u}) + \nabla \cdot (\rho \vec{u}\vec{u}) = \mu \nabla^2 \vec{u} - \nabla P + \rho \vec{g} + \vec{S} \tag{2}$$

$$\frac{\partial}{\partial t}(\rho H) + \nabla \cdot (\rho \vec{u} H) = \nabla \cdot (k \nabla T) \tag{3}$$

In the above equations, ρ is the density of fluid, t is time, g is the gravitational acceleration and $\vec{u}$ is the velocity vector. S is the source term which is calculated as:

$$S = A_{mushy} \frac{(1-\gamma)^2}{\gamma^3 + \varepsilon} \vec{u} \tag{4}$$

The parameter A_{mushy} is the mushy zone constant and assigning higher amount for this parameter accelerates the velocity reduction to zero during the solidification process. γ is the liquid volume fraction of the cell. ε is a small value (0.001) to avoid mathematical singularity when the whole material in the cell has solidified and γ equals to zero. In energy equation, "H" is the enthalpy which consists of sensible enthalpy and latent heat and is calculated as:

$$H = h + \Delta H \tag{5}$$

In which "h" is sensible enthalpy and is expressed as:

$$h = h_{ref} + \int_{T_{ref}}^{T} C_p \Delta T \tag{6}$$

where h_{ref} is a reference enthalpy associated to the reference Temperature (T_{ref}) and ΔH is the latent heat which is expressed as:

$$\Delta H = \gamma L_h \tag{7}$$

The liquid volume fraction in the above equations is calculated as:

$$\gamma = \begin{cases} 0 & if \quad T < T_s; \\ \dfrac{T - T_s}{T_l - T_s} & if \ T_s < T < T_l; \\ 1 & if \quad T_l < T; \end{cases} \tag{8}$$

In order to take the buoyancy driven convection flow into account, the boussinesq approximation is adopted. According to this method, the term of density in the momentum equation is calculated as:

Table 1
Thermo-physical properties of lauric acid [40].

Parameter	Value
Specific heat capacity solid/liquid (kJ/kg.K)	2.18/2.39
Melting temperature range (°C)	43.5–48.2
Latent heat of fusion (kJ/kg)	187.21
Thermal conductivity solid/liquid (W/m.K)	0.16/0.14
Density solid/liquid (kg/m^3)	940/885

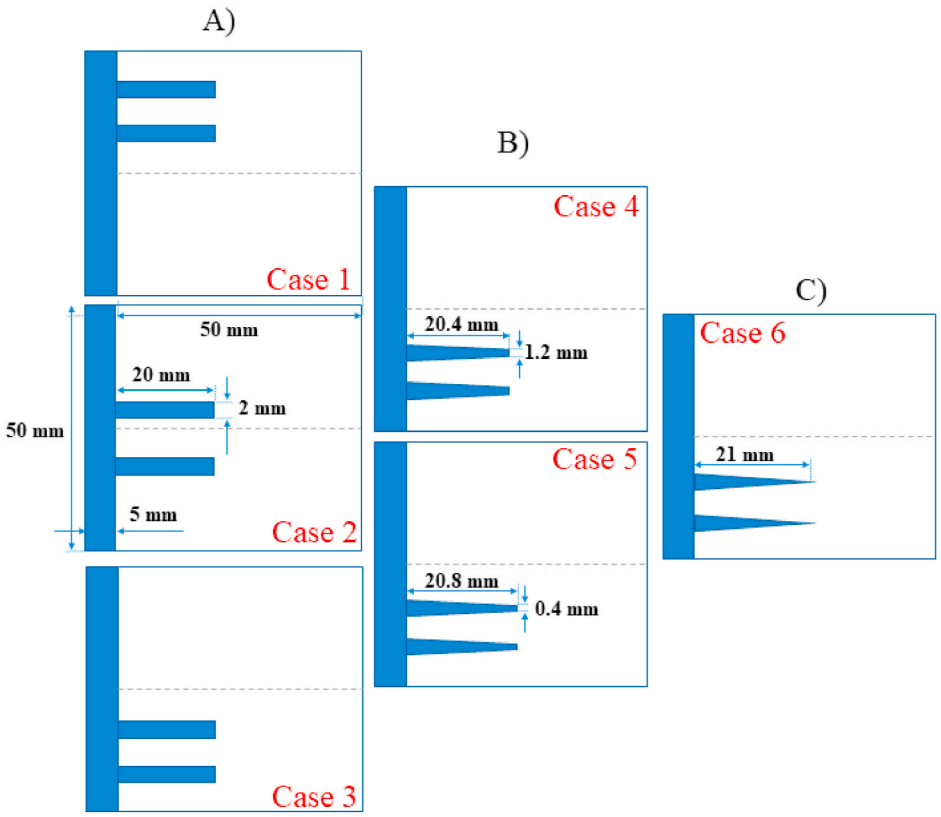

Fig. 1. Presentation of different stages and cases considered at present study; A) effect of location of fins, rectangular fin; B and C effect of shape of fins, trapezoidal and triangular fin.

$$\rho = \frac{\rho_l}{\beta(T - T_l) + 1} \tag{9}$$

where β is the thermal expansion coefficient and T_0 is the operating temperature.

The numerical methods used to solve the governing equations are as follows: The SIMPLE scheme is used for the pressure velocity coupling while PRESTO is used for pressure corrections equations and the second order upwind method has been used for discretization of the momentum and energy equations. The convergence was achieved when the residuals reduce below 10^{-4} for the continuity equation and 10^{-5} for momentum and energy equations.

2.3. Validation

The accuracy of the data achieved in this study was validated against the experimental data of Kamkari et al. [42] The model for validation is the melting of lauric acid as PCM in a rectangular enclosure which is isothermally being heated from the left side wall while the other walls have been insulated. The melt fraction against time in this work and the work of Kamkari et al. [42] have been compared in Fig. 2 A. As shown, the numerical data are in good agreement with the experimental data as the greatest deviation is observed at the end of the melting process which is about 6% which shows the reliability of the numerical data. Despite the melting fraction which represented the quantitative data, a set of contours have also been presented for a better comparison between numerical results and experimental results of Kamkari et al. [42]. Fig. 2 B presents the contours of melt fraction for 5 different melting times for both experimental and numerical study. Looking at Fig. 2 B, it could be observed that there is a very good agreement between the numerical results of the present study and the experimental results of the paper published by Kamkari et al. [42].

2.4. Mesh and time step independency analysis

Another aspect of evaluating the credibility of any numerical study is to check the independence of results to the cell numbers and time step. For checking the mesh independency analysis, three different cell numbers of 8569, 17,300 and 35,265 were considered. It was found that there was no significant difference between the results of melt fraction during the melting time associated with three cell numbers. Consequently, the cell number of 17,300 was considered for the rest of this study.

Furthermore, for the time independency analysis, three-time steps of 0.5s, 0.2s and 0.05 were considered. The melt fraction results

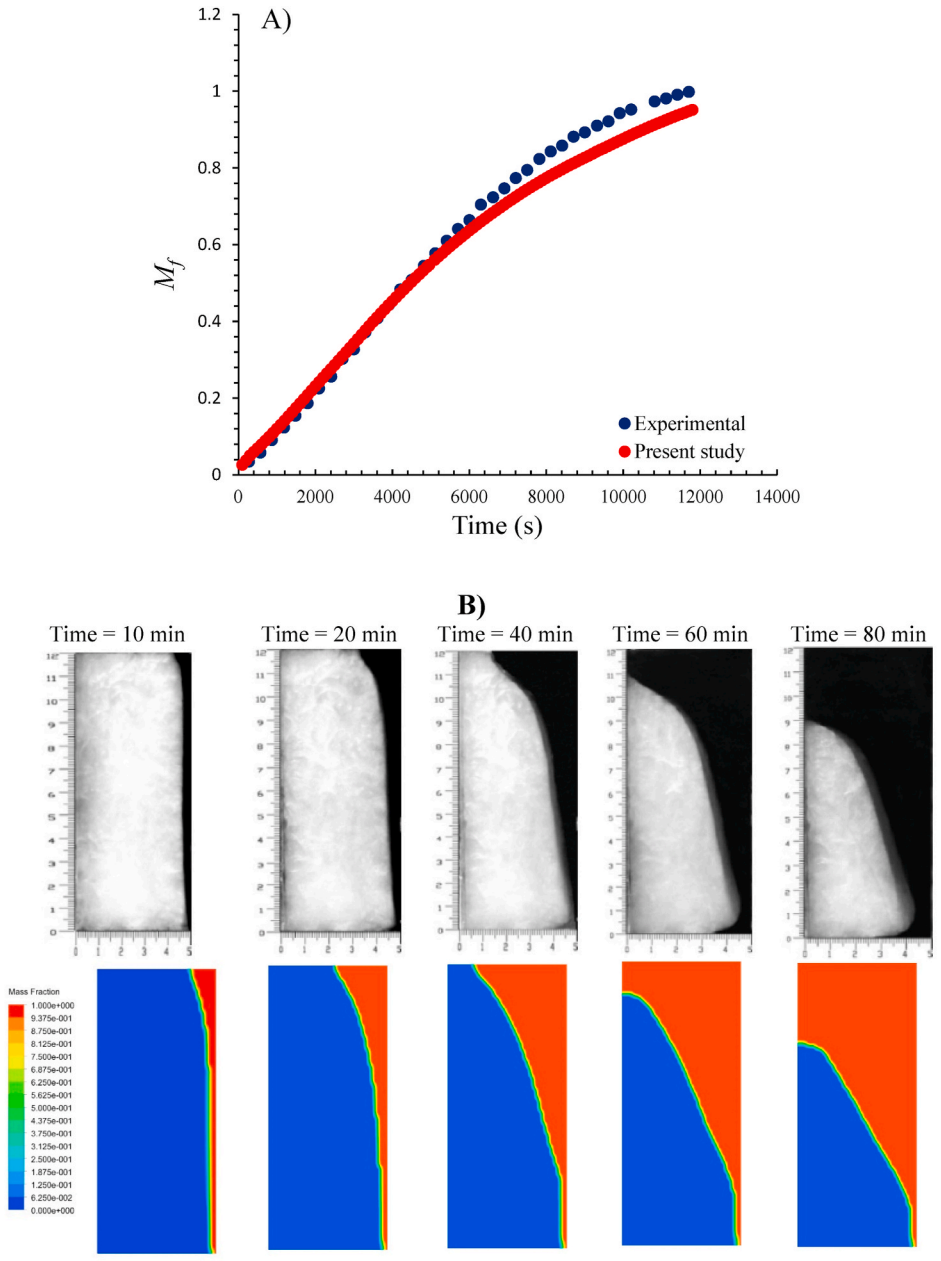

Fig. 2. Comparison of melt fraction results (A) and contours (B) of present study and the experimental study performed by Kamkari et al. [42].

associated with these three-time steps are presented in Fig. 3. It could be observed that there is no significant difference between the melt fraction results associated with the considered time steps. It is worth mentioning that for the rest of the study the time step of 0.2 was considered.

3. Results and discussion

3.1. Melt fraction analysis

In this section, the effect of fin position and fin shape on the improvement of the melting process is discussed. A very important parameter that could clearly present the effect of the mentioned parameters on the enhancement of the melting process is the melt fraction (M_f). The melt fraction is defined by equation (10). In this formula, the $S_{[T>321.35K]}$ is the area that has reached the melting temperature and is in the liquid form. The $S_{initial}$, is the Solid surface at the beginning of the process.

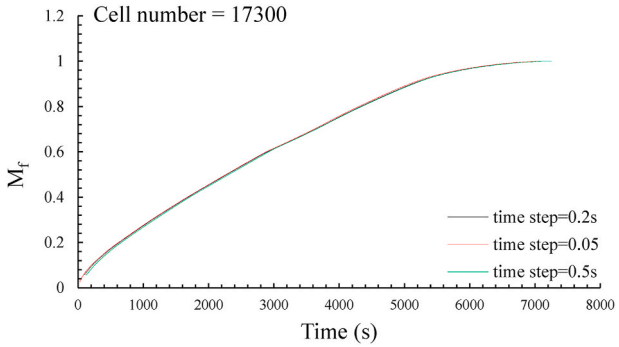

Fig. 3. Time independency checking at time steps of 0.5, 0.2 and 0.05.

$$M_f = \iint \frac{S_{[T>321.35K]}}{S_{initial}} dxdy \tag{10}$$

Fig. 4 A, presents the variation of M_f vs time for different cases considered in this study. As presented, up to t = 1000s, all cases with fins have a linear form of melt fraction with a very sharp slope. After t = 1000s, the melt fraction finds a curvy form in all cases with a reduction in their slope. The highest declining rate is related to case 1, at which the form of the fin was rectangular and was located at the upper half of the PCM enclosure. Between t = 1000s and t = 2000s, the declining slope of the rest of the cases (case 2 to case 6) almost remains constant. At t = 2000s, case 2, finds a bit more declining slope. It is observed that cases 4 and 5 have almost the same rate of melting. However, when case 5 (trapezoidal fin with a smaller fin head) is used, it is found that the rate of declining slope reduces significantly, when compared to other cases. The lowest declining slope is related to case 6, in which fins were located at the lower half of the PCM enclosure and had a triangular form. Consequently, case 6 is the first one that has reached the melting fraction of 1. The aforementioned explanations are schematically presented in Fig. 6. Looking to Fig. 4 B, it could be observed that the cases with fins located at the lower half of the enclosure, melt more quickly than the cases with fins at the middle of the enclosure or at the upper half of the PCM enclosure. This phenomenon could be explained by considering the isotherm contours presented in Fig. 4C. Looking to diagrams associated with cases 1 to 3 of Fig. 4C, it could be found that for case no. 1, at t = 500s, 1000s and 2000s, the area of the upper part of the enclosure that has reached the maximum temperature is more than that in cases 2 and 3. Since these areas are located at the highest part of the enclosure [43], the melted PCM could not move (the movement of melted PCM material is due to the buoyancy forces, and when it gets trapped between the and upper wall of the enclosure it could not have significant movements) [44]. Consequently, the temperature of this part increases significantly and the thermal energy becomes trapped in this area. However, when the fins are located at lower positions (cases 2 and 3), the melted PCM has the space and potential of moving in a vertical direction. Indeed, when the PCM material gets melted, due to the difference in density, the buoyance effect forces the melted parcels to move in a vertical direction and free convection occurs [45]. In this movement, melted parcels transfer their thermal energy to the surrounding PCM which leads to better heat transfer within the enclosure and faster melting of the PCM. When comparing case 3 with cases 2 and 1, it could be realized that this case has a faster melting process than the two others. Looking at isotherm contours associated with case 3 in Fig. 4C, it could be observed that when the fins are located at the lower half, the area with maximum temperature is the minimum when compared with cases 2 and 1. Instead, there are more areas that have reached the melting temperature.

As mentioned before, cases 4 to 6 are considered to investigate the effect of fin shape. Two trapezoidal forms and one triangular form were used. It is obvious that case 4 has a little better performance in the melting process than case 3. Fig. 4 A and 4 B reveal that cases 5 and 6 have better performance than case 3. It is found from the diagrams in Fig. 4C that when the shape of fins changes from rectangular to trapezoidal form, the area with maximum temperature between the two fins becomes less than that of the rectangular fins. By changing the trapezoidal form to triangular form, the decrement in the area with maximum temperature increases. This means that changing the shape of fins to the trapezoidal and rectangular form reduces the trapped energy between the fins. When this trapped energy is released, two main phenomena occur. Firstly, when the area around the fins fills with a material having a temperature less than the maximum, the heat transfer procedure occurs at a faster pace. Secondly, during the movement of the materials, the energy becomes transferred to the other parts of the material. So, melting happens faster.

3.1.1. Total saved time

Fig. 5 A presents the total melting time for the various cases considered in this study. As indicated in this figure, by changing the location of the double fins (case 1 to case 3), the total melting time decreases. However, comparing case 4 (first trapezoidal fin, located at the lower half of the enclosure) and case 3 (rectangular fin, located at the lower half of the enclosure) it is observed that there is no significant difference between the melting time of the aforementioned cases. By looking at case 5 and case 6, it is revealed that in contrary to case 4, the total melting time has decreased more significantly. The minimum melting time was about 7100s and was related to case 6, at which the triangular double fins were located at the lower half of the PCM enclosure.

Fig. 5 B and C presents the total saved time achieved by applying the aforementioned type of fins to the PCM enclosure. Fig. 5 B presents the saved time at which the cases were compared to the base model. However, in Fig. 5C, the base model was considered to be case 3, the aim of this figure is to present the effect of fin shape. Looking at Fig. 5 B, it could be seen that amongst the cases at which the

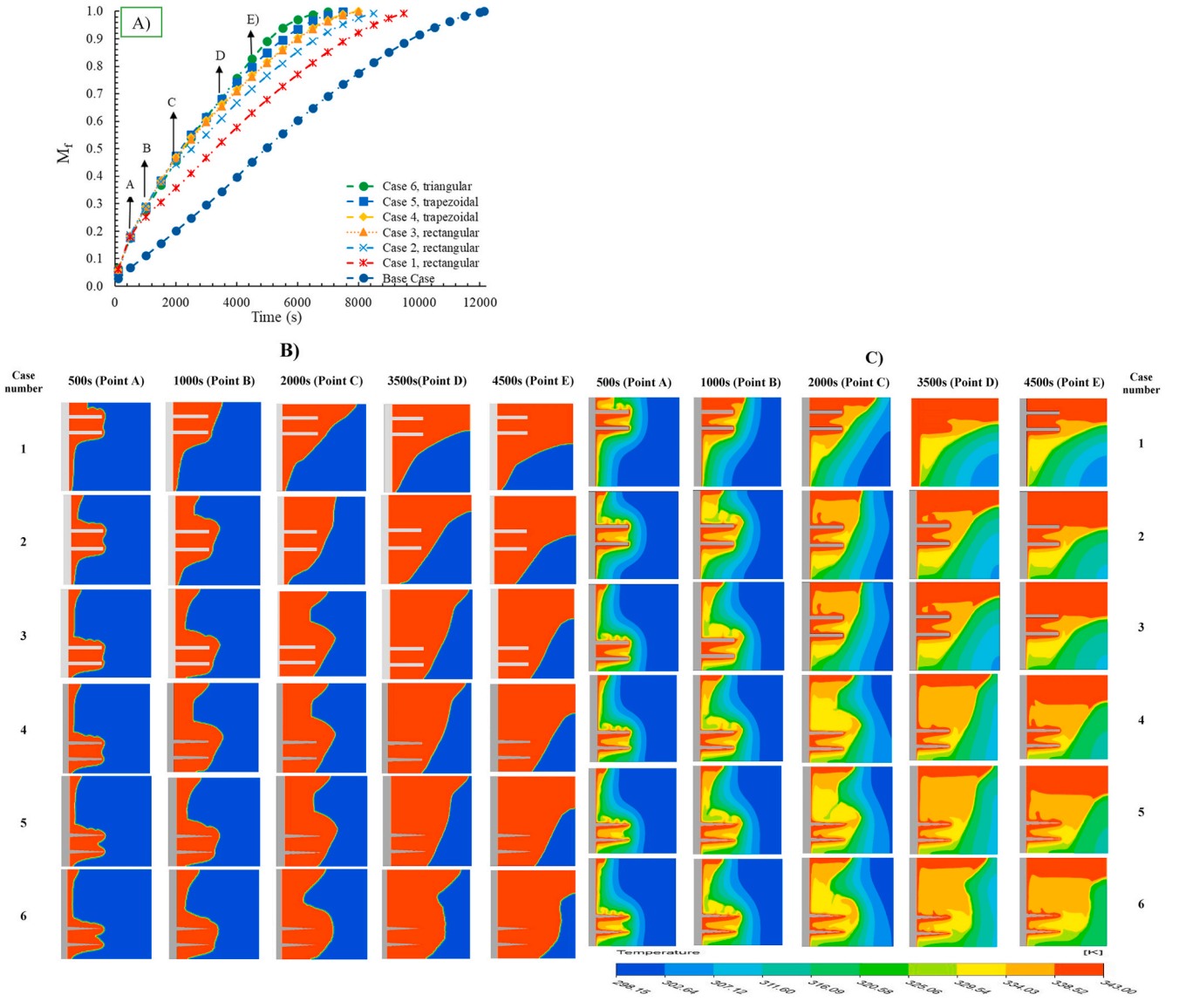

Fig. 4. A) Variation of melt fraction vs time, B) Melt fraction counters for different cases at critical seconds, C) Isotherm contours for different cases at critical seconds.

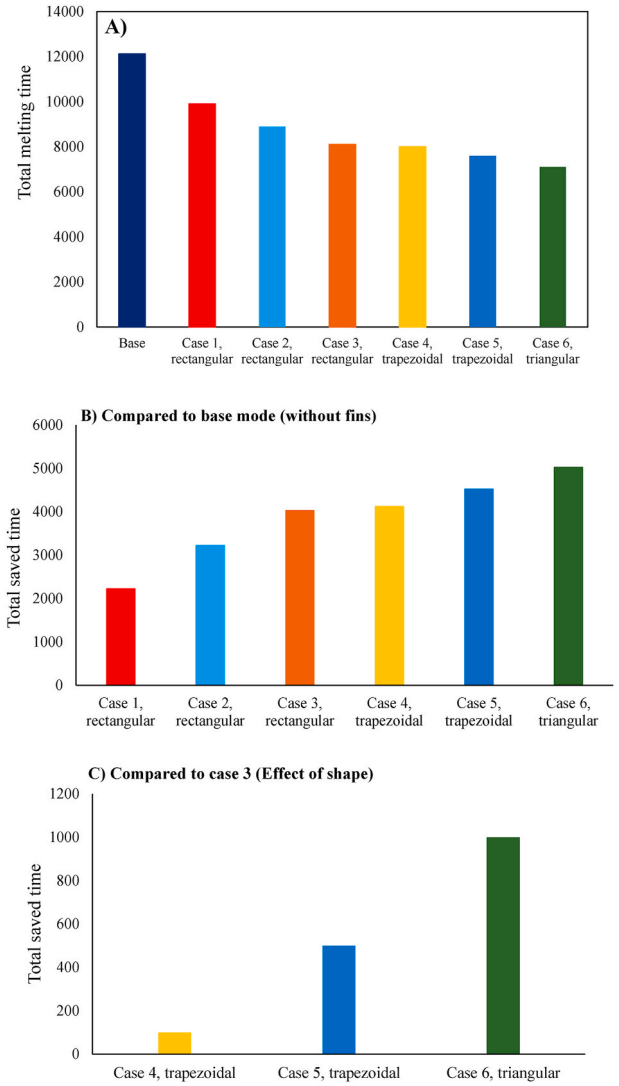

Fig. 5. A) Total melting time for different cases considered in this study, B) Total saved time when compared to base mode, C) Total saved time when compared to case 3 (Effect of shape).

effect of location was examined the maximum saved time was related to case 3. Consequently, by presenting Fig. 5C, the authors intended to indicate the effect of changing the shape of fins. By looking at Fig. 5 B, it could be seen that the maximum saved time is 5020s. Also Fig. 5C reveals that a maximum saved time of about 1000s could be observed.

3.1.2. Enhancement ratio

The enhancement ratio is another quantitative parameter that could be used to evaluate the performance of any mechanism used for improving the performance of PCM. In this study, two different formulations are used for the enhancement ratio. The first one was Er_0 at which the cases 1 to 6 were compared with finless enclosure and is defined as below.

$$Er_0 = \left(\frac{m_{f,\ with\ fin}}{m_{f,\ without\ fin}} - 1\right) \times 100 \tag{11}$$

The second definition is Er_s and is calculated by equation (12). In this formula, the case 3 is considered to be as the base case. Indeed, this parameter is defined to evaluate the effect of fin shape on the melting performance of the PCM enclosure.

$$Er_s = \left(\frac{m_{f,\ case\ 4-6}}{m_{f,\ case\ 3}} - 1\right) \times 100 \tag{12}$$

It is found in Fig. 6 A, that up to t = 500s, the Er_0 increases with time for all cases. the maximum enhancement ratio (Er_0) was about 177% and was occurred at t = 500s and was related to case 2 which had rectangular double fins that were located at the lower half of

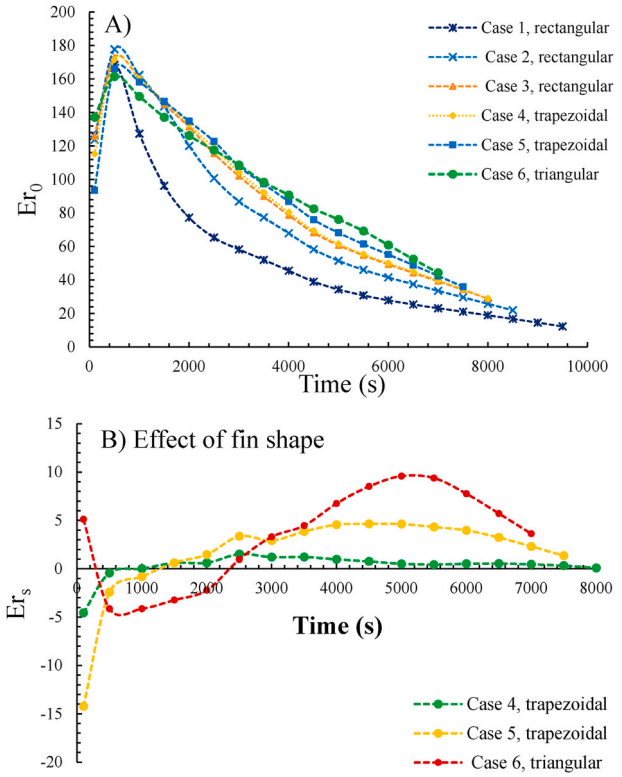

Fig. 6. A) Variation of Er_0 (Enhancement in melting when compared to finless mode) versus time B) Variation of Er_s (Enhancement in melting when compared to case 3) vs time.

the enclosure. Up to t = 3000s the Er_0 related to case 6 is less than most cases, however after this time, the enhancement ratio of case 6 becomes more than other cases.

For the comparison between the different shapes of the fins presented in this study the Er_s is provided in Fig. 6 B. As presented up to t = 500s, the case 6 (triangular fin) has better performance than the cases related to rectangular fin. However, from t = 500s to t = 1500s all cases of 4–6 have negative values of Er_s, denoting that in this period the performance of rectangular fin is better than trapezoidal and triangular fin at the considered conditions. This remains constant for the case 6 up to t = 2500s. after this time a great enhancement could be seen in case 6 which reaches up to %9.38% increment in the values of Er_s. After t = 2500s, the case 6 has the best performance until the end of the melting process.

3.2. Thermal properties

3.2.1. PCM velocity analysis

PCM melting process is affected by buoyancy induced flows. Since these flow streams could transfer the thermal energy, they play a very important role in the melting process. Velocity contours could be useful for better understanding of the velocity field. Fig. 7 A, presents the velocity contours colored by velocity magnitude. It is found that in cases in which the fins are located at the lower half of the enclosure, the velocity vectors are more dens, besides the velocity vectors have higher values of velocity quantities. For example, if we compare case 3 with case 1 and 2 at t = 2000s, it could be easily observed that the case 3, has denser velocity vectors than case 2 and 1. Besides, at t = 2000s, there are more areas in case 3, that the velocity vectors are colored with yellow and red meaning that these parts have higher velocities than those related to case 1 and 2. The greater velocity magnitude in these areas leads to better circulation of melted PCM, as a result the more thermal energy transfers to other sides and the thermal energy doesn't get trapped in a certain area. Looking at t = 4500s, it could be easily found that the case 3 has more melted area than the cases 1 and 2. On the other hand, when comparing the cases 4 to 6 with case 3, it could be seen that in case 6 and 5, the density of velocity vectors are more than case 3. Also, the melt fraction contours show that after t = 2000s, there is significant difference in the melt fraction of case 6 when compared to other cases. By looking at velocity contours, it is observed that the free convection resulted from the melted PCM has enhanced the transfer. It is worth mentioning that these motions induce vortices in the flow stream and enhance the melting rate.

The maximum velocity is an indicator of intensity of free convective heat transfer, since it is a result of buoyancy induced flow. Actually, as the density difference increases, the buoyancy induced flows to get more powerful which enhances the heat transfer in the PCM. The variation of maximum velocity versus time is presented in Fig. 7 B. As indicated in this figure there are three main areas that present the regions of heat transfer convection as could be seen before t = 500s, the maximum velocities have very low values. In this

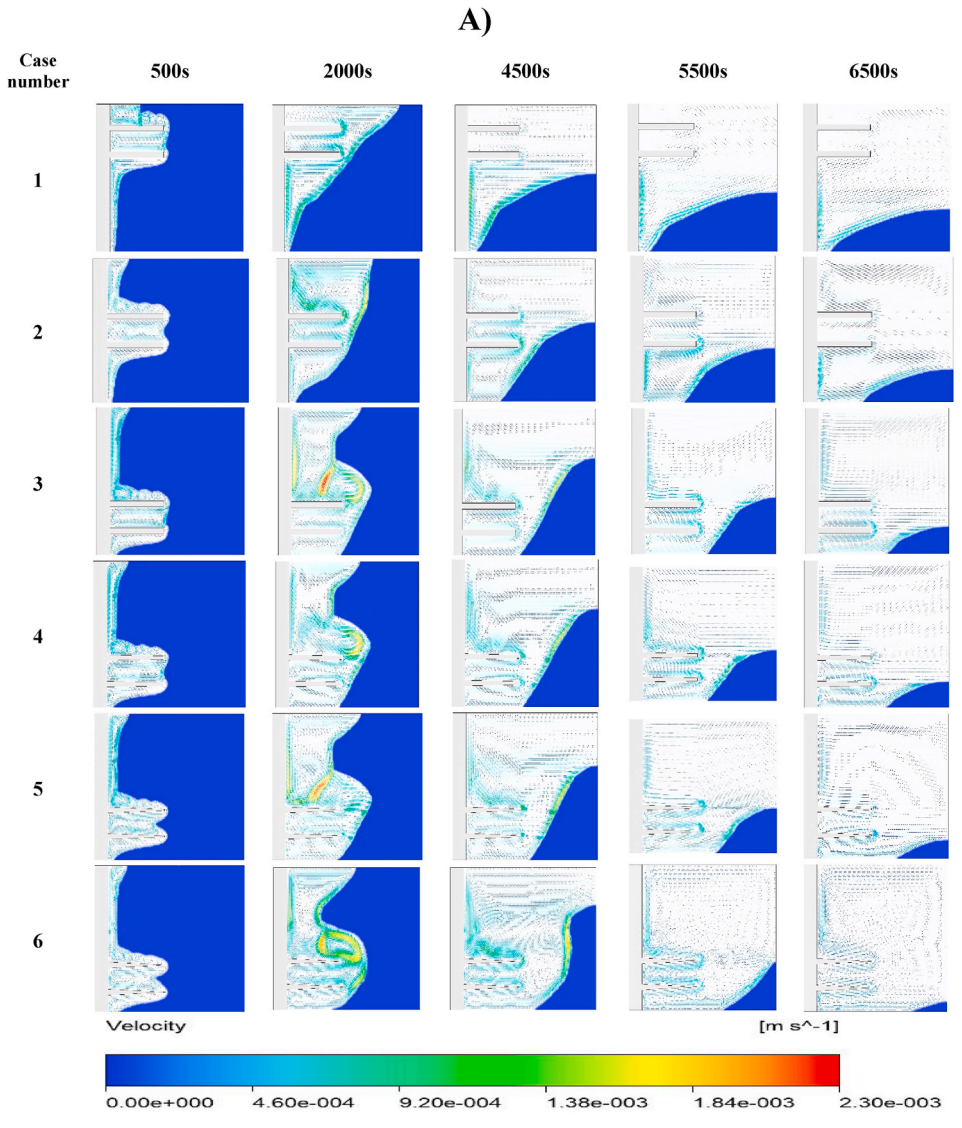

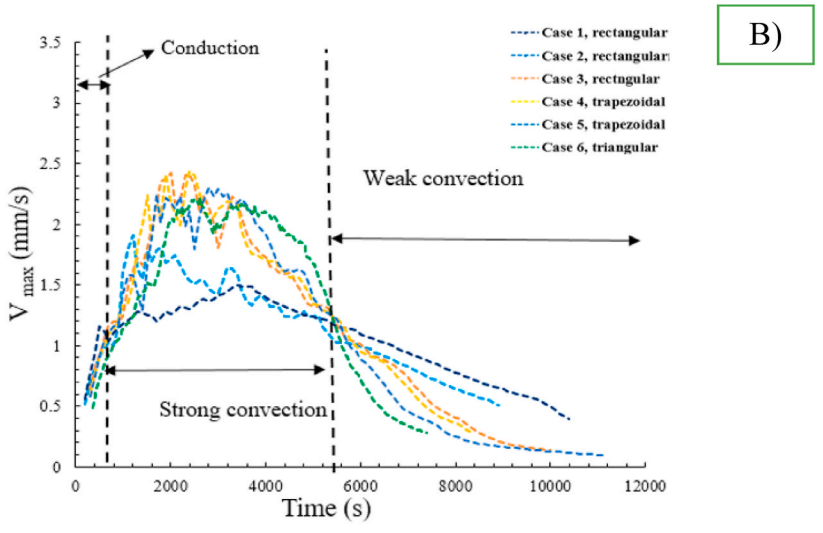

(caption on next page)

Fig. 7. A) Presentation of velocity contours for different cases considered in this study, B) Variation of maximum velocity vs time.

period the dominant heat transfer mechanism is the conduction. Over time the buoyancy induced flow streams appear. In the period of t = 500s to t = 5700s, the velocity values are in the range of strong convection. After t = 5700s the range of values for the maximum velocity demonstrates existence of weak convection. Looking at Fig. 13, it could be seen that from the time t = 500s to about t = 3000s all cases have positive slope. In this period cases 3 and 4 have the most values of maximum velocity. After t = 3000s, all cases have a negative slope and the values of maximum velocity begin to reduce. Up to t = 5700s the case 6 has the minimum declining slope and the maximum velocities associated with case 6 have the maximum values meaning that in this period case 6 has the most powerful buoyancy induced flow. However, after t = 5600s case 6 finds a bit more declining slope finds the lowest values of maximum velocity. It is noteworthy, that time interval at which case 6 has the most values of maximum velocity was longer than other cases (during strong convection) this is why the case 6 has the best overall performance amongst other cases considered in the present study.

3.2.2. Nusselt number

Nusselt number as an indicator of heat transfer rate has an important role on evaluating any thermal system. The Nusselt number in this study is calculated as follows:

$$\overline{Nu}(t) = \frac{\overline{h}(t) L_c}{k} \tag{13}$$

At which $\overline{h}(t)$ is the surface averaged heat transfer rate and the $L_{c,}$ is characteristic length. In this study the length of container was considered to be as the characteristic length L_c. The $\overline{h}(t)$ is calculated as follows [17]:

$$\overline{h}(t) = \frac{Q_{total}(t)}{A_w (T_w - T_m) \Delta t} \tag{14}$$

At which the $Q_{total}(t)$ is the total heat transferred to PCM during the time period of Δt. $T_w$and T_m are the surface average temperature and PCM mean temperature, respectively. Also, A_w is the area at which heat has been transferred to PCM.

Fig. 14, shows the Nusselt number vs dimensionless time (Fo). The Fourier number as the dimensionless time is defined as follows:

$$Fo = \frac{\alpha t}{l^2} \tag{15}$$

where t is the time, α is the thermal diffusivity and L is the characteristic length.

Looking at Fig. 8, it could be found that at the beginning of the melting process when conduction is the dominant heat transfer mechanism, the Nusselt number associated with all cases has the greatest value. In this period the melted PCM has the smallest thickness. Through the melting process the thickness of melted layer increases which results in increment of convective thermal resistance so the Nu number decreases very fast. After Fo = 0.02 the declining slope of Nu number curves decreases significantly, in this period the buoyancy induced flow was created and contributed to better heat transfer rate. This procedure continues until Fo = 0.15. It could be concluded that between Fo = 0.02 and Fo = 0.15 the strong convection was the dominant form of heat transfer. After Fo = 0.15 the Nu number curves find a bit sharper declining slop. From Fig. 13, it could be understood that after Fo = 0.15 the weak convection becomes the dominant form of the heat transfer. As presented in Fig. 8, case 6 has the lowest values of maximum velocity leading to the weakest convection form of the heat transfer. By looking at Fig. 8, it could be seen that after Fo = 0.15 the declining slope of case 6 is the most sharper one. This is an agreement with the behavior of maximum velocity curve presented in Fig. 7 B. It should be noted that despite the convective streams, higher thermal performance of triangular fins also contributes to higher values of Nu of case 6 from beginning of melting process until Fo = 0.15. For example, in Fig. 7 B, it was found that between t = 500s and t = 3000s case 6 has weaker convective streams, however, it is observed that during the mentioned time interval the best Nu number is related to case 6. This is due to better thermal performance of triangular-shaped fins.

4. Conclusions

At the present study, a vertical PCM enclosure having the dimensions of $50mm \times 50\ mm$ was considered to evaluate the effect of position and shape of double fins on the melting performance of a PCM enclosure. The Lauric acid was considered as the PCM material. The heated wall was set to have a temperature of 343 K. The Enthalpy porosity method was used for simulating the melting process. Six different cases were considered. Three of the considered cases were related to evaluating the effect of fin position while the other three cases were dedicated to evaluate the effect fin shape on melting enhancement of PCM. For evaluation of the fin position rectangular double fins having same length were considered. Also two different trapezoidal and one triangular shaped fin were used. The results demonstrated that when the fins are located at the lower half the enclosure, best melting performance could be achieved. The main findings of the present study are stated at the following:

- ✓ For the position of fins, when the fins located at the lower half have the best performance. It was found that when rectangular double fins are located at lower half of the enclosure, up to 1800s less melting time could be achieved (comparison between case 3 and case 1).

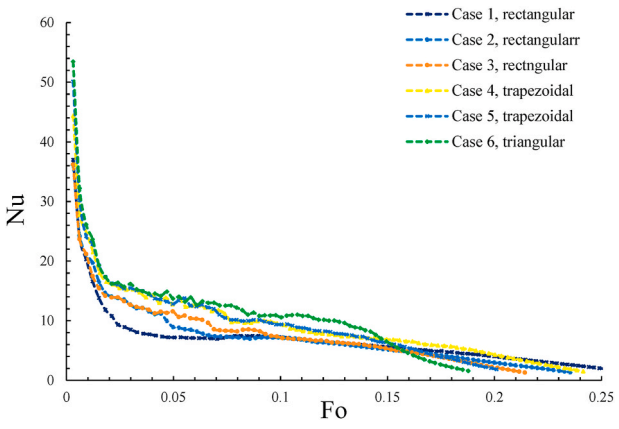

Fig. 8. Variation of Nu number vs Fo number.

- ✓ For the effect of fin shape, the triangular fins presented the best results. It was found that the triangular fins (case 6) could save up to 1000s in the whole melting process. Case 6 showed the fastest melting speed.
- ✓ It was found that during the strong convection period, from the second of 500s to about 3000s the maximum velocity associated with all cases increases. During this period the highest values of V_{max} were related to case 4, denoting this point that case 5 has better convective heat transfer at the mentioned interval.
- ✓ The time intervals at which the cases 4 and 6 had the most powerful convective heat transfer were 2500s and 2700s, respectively. Since, the time interval for case 6 was more than case 4, the overall performance of case 6 (triangular double fin) was the better one.
- ✓ From the beginning of the melting process and up to Fo = 0.15, the maximum Nu numbers values were related to case 6. Both the effect of well free convection and better thermal performance of triangular fins were involved in the better thermal performance of PCM enclosure with double triangular fin located at the lower half of the enclosure.

CRediT authorship contribution statement

Nazaruddin Sinaga: Resources, Formal analysis, Investigation. **Hazim Moria:** Writing - review & editing, Investigation. **Kottakkaran Sooppy Nisar:** Resources, Formal analysis. **Cuong Manh Vu:** Writing - review & editing, ConceptualizationConceptualism. **Behzad Heidarshenas:** Writing - review & editing, Methodology, Formal analysis. **Akbar Arsalanloo:** Software, Post processing. **Mohammad Mehdizadeh Youshanlouei:** Writing - original draft, Mesh generation.

Declaration of competing interest

No conflict of interest.

References

[1] B. Zhu, B. Su, Y. Li, Input-output and structural decomposition analysis of India's carbon emissions and intensity, 2007/08 – 2013/14, Appl. Energy 230 (2018) 1545–1556, https://doi.org/10.1016/j.apenergy.2018.09.026.
[2] L. He, Y. Chen, J. Li, A three-level framework for balancing the tradeoffs among the energy, water, and air-emission implications within the life-cycle shale gas supply chains, Resour. Conserv. Recycl. 133 (2018) 206–228, https://doi.org/10.1016/j.resconrec.2018.02.015.
[3] G. Wang, Y. Yao, Z. Chen, P. Hu, Thermodynamic and optical analyses of a hybrid solar CPV/T system with high solar concentrating uniformity based on spectral beam splitting technology, Energy 166 (2019) 256–266, https://doi.org/10.1016/j.energy.2018.10.089.
[4] Y. Zhang, X. Zhang, M. Li, Z. Liu, Research on heat transfer enhancement and flow characteristic of heat exchange surface in cosine style runner, Heat Mass Tran. 55 (2019) 3117–3131, https://doi.org/10.1007/s00231-019-02647-5.
[5] R. Yousefnejad, N. Atabaki, M. Chiao, An algorithm for designing a cooling system for photovoltaic panels, Sol. Energy 194 (2019) 450–460, https://doi.org/10.1016/j.solener.2019.10.031.
[6] C. Cai, X. Wu, W. Liu, W. Zhu, H. Chen, J.C.D. Qiu, C.-N. Sun, J. Liu, Q. Wei, Y. Shi, Selective laser melting of near-α titanium alloy Ti-6Al-2Zr-1Mo-1V: parameter optimization, heat treatment and mechanical performance, J. Mater. Sci. Technol. 57 (2020) 51–64, https://doi.org/10.1016/j.jmst.2020.05.004.
[7] J. Lin, J. Hu, W. Wang, K. Liu, C. Zhou, Z. Liu, S. Kong, S. Lin, Y. Deng, Z. Guo, Thermo and light-responsive strategies of smart titanium-containing composite material surface for enhancing bacterially anti-adhesive property, Chem. Eng. J. (2020) 125783, https://doi.org/10.1016/j.cej.2020.125783.
[8] S. Chen, M.K. Hassanzadeh-Aghdam, R. Ansari, An analytical model for elastic modulus calculation of SiC whisker-reinforced hybrid metal matrix nanocomposite containing SiC nanoparticles, J. Alloys Compd. 767 (2018) 632–641, https://doi.org/10.1016/j.jallcom.2018.07.102.
[9] F. Agyenim, N. Hewitt, P. Eames, M. Smyth, A review of materials, heat transfer and phase change problem formulation for latent heat thermal energy storage systems (LHTESS), Renew. Sustain. Energy Rev. 14 (2010) 615–628, https://doi.org/10.1016/j.rser.2009.10.015.
[10] T. Ni, Y. Yao, H. Chang, L. Lu, H. Liang, A. Yan, Z. Huang, X. Wen, LCHR-TSV: novel low cost and highly repairable honeycomb-based TSV redundancy architecture for clustered faults, IEEE Trans. Comput. Des. Integr. Circuits Syst. 39 (2020) 2938–2951, https://doi.org/10.1109/TCAD.2019.2946243.
[11] Z.-G. Shen, L.-L. Tian, X. Liu, Automotive exhaust thermoelectric generators: current status, challenges and future prospects, Energy Convers. Manag. 195 (2019) 1138–1173, https://doi.org/10.1016/j.enconman.2019.05.087.
[12] A. Crespo, C. Barreneche, M. Ibarra, W. Platzer, Latent thermal energy storage for solar process heat applications at medium-high temperatures – a review, Sol. Energy 192 (2019) 3–34, https://doi.org/10.1016/j.solener.2018.06.101.

[13] T. Khadiran, M.Z. Hussein, Z. Zainal, R. Rusli, Advanced energy storage materials for building applications and their thermal performance characterization: a review, Renew. Sustain. Energy Rev. 57 (2016) 916–928, https://doi.org/10.1016/j.rser.2015.12.081.
[14] F. Zhu, C. Zhang, X. Gong, Numerical analysis on the energy storage efficiency of phase change material embedded in finned metal foam with graded porosity, Appl. Therm. Eng. 123 (2017) 256–265, https://doi.org/10.1016/j.applthermaleng.2017.05.075.
[15] T. Ni, Q. Xu, Z. Huang, H. Liang, A. Yan, X. Wen, A cost-effective TSV repair architecture for clustered faults in 3D IC, IEEE Trans. Comput. Des. Integr. Circuits Syst. (2020) 1, https://doi.org/10.1109/TCAD.2020.3025169.
[16] A. Acir, M.E. Canli, Investigation of fin application effects on melting time in a latent thermal energy storage system with phase change material (PCM), Appl. Therm. Eng. (2018), https://doi.org/10.1016/j.applthermaleng.2018.09.013.
[17] C. Ji, Z. Qin, S. Dubey, F.H. Choo, F. Duan, Simulation on PCM melting enhancement with double-fin length arrangements in a rectangular enclosure induced by natural convection, Int. J. Heat Mass Tran. 127 (2018) 255–265, https://doi.org/10.1016/j.ijheatmasstransfer.2018.07.118.
[18] X. Jinlong, L.H. Mun, X. Jianhua, Numerical study of thermally optimized metal structures in a Phase Change Material (PCM) enclosure, Appl. Therm. Eng. 148 (2019) 825–837, https://doi.org/10.1016/j.applthermaleng.2018.11.111.
[19] X. Jia, X. Zhai, X. Cheng, Thermal performance analysis and optimization of a spherical PCM capsule with pin- fins for cold storage, Appl. Therm. Eng. 148 (2019) 929–938, https://doi.org/10.1016/j.applthermaleng.2018.11.105.
[20] M. Arıcı, E. Tütüncü, M. Kan, H. Karabay, Melting of nanoparticle-enhanced paraffin wax in a rectangular enclosure with partially active walls, Int. J. Heat Mass Tran. 104 (2017) 7–17, https://doi.org/10.1016/j.ijheatmasstransfer.2016.08.017.
[21] L. Colla, L. Fedele, S. Mancin, L. Danza, O. Manca, NANO-PCMS for enhanced energy storage and passive cooling applications, Appl. Therm. Eng. (2016), https://doi.org/10.1016/j.applthermaleng.2016.03.161.
[22] M. Ghalambaz, A. Doostani, E. Izadpanahi, A.J. Chamkha, Phase-change heat transfer in a cavity heated from below : the effect of utilizing single or hybrid nanoparticles as additives, 0, J. Taiwan Inst. Chem. Eng. (2017) 1–12, https://doi.org/10.1016/j.jtice.2017.01.010.
[23] M. Fang, G. Chen, Effects of different multiple PCMs on the performance of a latent thermal energy storage system, Appl. Therm. Eng. 27 (2007) 994–1000, https://doi.org/10.1016/j.applthermaleng.2006.08.001.
[24] M.M. Farid, A. Kanzawa, Thermal performance of a heat storage module using PCM ' s with different melting Temperatures : mathematical modeling, J. Sol. Energy Eng. 111 (2013).
[25] A.M. Sefidan, M. Taghilou, M.P. Mohammadpour, A. Sojoudi, Effects of different parameters on the discharging of double- layer PCM through the porous channel, Appl. Therm. Eng. (2017), https://doi.org/10.1016/j.applthermaleng.2017.05.131.
[26] R. Baby, C. Balaji, Experimental investigations on thermal performance enhancement and effect of orientation on porous matrix fi lled PCM based heat sink, Int. Commun. Heat Mass Tran. 46 (2013) 27–30, https://doi.org/10.1016/j.icheatmasstransfer.2013.05.018.
[27] M. Sheikholeslami, R. Haq, A. Shafee, Z. Li, Heat transfer behavior of nanoparticle enhanced PCM solidification through an enclosure with V shaped fins, Int. J. Heat Mass Tran. 130 (2019) 1322–1342, https://doi.org/10.1016/j.ijheatmasstransfer.2018.11.020.
[28] M. Sheikholeslami, Numerical simulation for solidification in a LHTESS by means of nano-enhanced PCM, J. Taiwan Inst. Chem. Eng. (2018) 1–17, https://doi.org/10.1016/j.jtice.2018.03.013, 0.
[29] A.A. Rabienataj Darzi, M. Jourabian, M. Farhadi, Melting and solidification of PCM enhanced by radial conductive fins and nanoparticles in cylindrical annulus, Energy Convers. Manag. 118 (2016) 253–263, https://doi.org/10.1016/j.enconman.2016.04.016.
[30] A. Arshad, H.M. Ali, M. Ali, S. Manzoor, Thermal performance of phase change material (PCM) based pin-finned heat sinks for electronics devices: effect of pin thickness and PCM volume fraction, Appl. Therm. Eng. 112 (2017) 143–155, https://doi.org/10.1016/j.applthermaleng.2016.10.090.
[31] S.F. Hosseinizadeh, F.L. Tan, S.M. Moosania, Experimental and numerical studies on performance of PCM-based heat sink with different configurations of internal fins, Appl. Therm. Eng. 31 (2011) 3827–3838, https://doi.org/10.1016/j.applthermaleng.2011.07.031.
[32] C. Ji, Z. Qin, Z. Low, S. Dubey, F.H. Choo, F. Duan, Non-uniform heat transfer suppression to enhance PCM melting by angled fins, Appl. Therm. Eng. 129 (2018) 269–279, https://doi.org/10.1016/j.applthermaleng.2017.10.030.
[33] X. Cao, Y. Yuan, B. Xiang, L. Sun, Z. Xingxing, Numerical investigation on optimal number of longitudinal fins in horizontal annular phase change unit at different wall temperatures, Energy Build. 158 (2018) 384–392, https://doi.org/10.1016/j.enbuild.2017.10.029.
[34] M.H. Joneidi, M. Rahimi, R. Pakrouh, R. Bahrampoury, Experimental analysis of Transient melting process in a horizontal cavity with different configurations of fins, Renew. Energy 145 (2020) 2451–2462, https://doi.org/10.1016/j.renene.2019.07.114.
[35] A. Abdi, V. Martin, J.N.W. Chiu, Numerical investigation of melting in a cavity with vertically oriented fins, Appl. Energy 235 (2019) 1027–1040, https://doi.org/10.1016/j.apenergy.2018.11.025.
[36] J. Xie, H.M. Lee, J. Xiang, Numerical study of thermally optimized metal structures in a Phase Change Material (PCM) enclosure, Appl. Therm. Eng. 148 (2019) 825–837, https://doi.org/10.1016/j.applthermaleng.2018.11.111.
[37] L.L. Tian, X. Liu, S. Chen, Z.G. Shen, Effect of fin material on PCM melting in a rectangular enclosure, Appl. Therm. Eng. 167 (2020), https://doi.org/10.1016/j.applthermaleng.2019.114764.
[38] Ç. Yıldız, M. Arıcı, S. Nižetić, A. Shahsavar, Numerical investigation of natural convection behavior of molten PCM in an enclosure having rectangular and tree-like branching fins, Energy 207 (2020), https://doi.org/10.1016/j.energy.2020.118223.
[39] S. Moreno, J.F. Hinojosa, I. Hernández-López, J. Xaman, Numerical and experimental study of heat transfer in a cubic cavity with a PCM in a vertical heated wall, Appl. Therm. Eng. 178 (2020) 115647, https://doi.org/10.1016/j.applthermaleng.2020.115647.
[40] H. Shokouhmand, B. Kamkari, Experimental investigation on melting heat transfer characteristics of lauric acid in a rectangular thermal storage unit, Exp. Therm. Fluid Sci. 50 (2013) 201–212, https://doi.org/10.1016/j.expthermflusci.2013.06.010.
[41] V.R. Voller, C. Prakash, A fixed grid numerical modelling methodology for convection-diffusion mushy region phase-change problems, Int. J. Heat Mass Tran. 30 (1987) 1709–1719, https://doi.org/10.1016/0017-9310(87)90317-6.
[42] B. Kamkari, H. Shokouhmand, F. Bruno, Experimental investigation of the effect of inclination angle on convection-driven melting of phase change material in a rectangular enclosure, Int. J. Heat Mass Tran. 72 (2014) 186–200, https://doi.org/10.1016/j.ijheatmasstransfer.2014.01.014.
[43] Y. Zhang, P. Huang, Influence of mine shallow roadway on airflow temperature, Arab. J. Geosci. 13 (2019) 12, https://doi.org/10.1007/s12517-019-4934-7.
[44] S.Y. Motlagh, M.M. Youshanloei, T. Safabakhsh, Numerical investigation of FHD pump for pumping the magnetic nanofluid inside the microchannel with hydrophobic walls, J. Brazilian Soc. Mech. Sci. Eng. 41 (2019) 237.
[45] E. Liu, L. Lv, Y. Yi, P. Xie, Research on the steady operation optimization model of natural gas pipeline considering the combined operation of air coolers and compressors, IEEE Access 7 (2019) 83251–83265, https://doi.org/10.1109/ACCESS.2019.2924515.